

Mathematical Modeling of Yellow Fever Transmission Dynamics with Multiple Control Measures.

Abstract

Yellow-fever disease remains endemic in some parts of the world despite the availability of a potent vaccine and effective treatment for the disease. This necessitates continuous research to possibly eradicate the spread of the disease and its attendant burden. Consequently, a deterministic model for Yellow-fever disease transmission dynamics within the human and vector population is considered. The model equilibrium solutions are obtained while the criteria for their existence and stability are investigated. The model is solved numerically using the fourth order Runge-Kutta scheme and the results are simulated for different scenarios of interest. Findings from the simulations show that the disease will continue to be prevalent in our society (no matter how small) as long as the immunity conferred by the available vaccine is not lifelong and the Yellow-fever infected mosquitoes continue to have unhindered access to humans. Thus, justifying the wisdom behind the practice of continuous vaccination and the use of mosquito net in areas of high Yellow-fever endemicity. However, it was equally found that the magnitude of the Yellow-fever outbreak can be remarkably reduced to a negligible level with the adoption of chemical or biological control measures which ensure that only mosquitoes with minimal biting tendency thrive in the environment.

Keywords: Yellow-fever, equilibrium solutions, disease prevalence, asymptotic stability, basic reproduction number.

1 Introduction

Outbreaks of infectious diseases have been a threat to human existence over time. It often culminates into loss of numerous lives while monumental amount of resources (money, human efforts, medical facilities and equipment, etc.) are deployed to put the spread of such disease under control or possibly eradicate it. Although, many infectious disease epidemic could be attributed to poor hygienic conditions, unhindered access of disease vector to the susceptible individuals, or human beings not taking appropriate and timely control measures to curtail the spread of such diseases. However, some of these diseases still spread with effective control measures in place; particularly in the case of vector-borne and air-borne diseases. In this paper, the focus shall be on Yellow-fever which is a vector-borne disease. This is imperative because the disease is currently endemic in some parts or whole of over forty different countries of the world while continuous proactive measures have to be in place to perpetually contain the disease.

Yellow fever (YF) is an acute viral infection caused by the bites of an infected female 'Aedes aegypti' mosquito [12]. The virus can be deposited in humans or any other primate by the mosquitoes; where it is then transmitted among humans through infected mosquitoes. Thereafter, the virus incubates in the infected individual for a duration of 3 to 6 days with patients exhibiting symptoms like mild fever, muscle pain with backache, headache, loss of appetite, jaundice, nausea, vomiting, and fatigue [12]. Nevertheless, these symptoms ceases after a maximum of four days while the patient may occasionally progress to the toxic phase of the infection which often results into death within a span of 7 – 10 days in 50% of such cases. Although, there is presently no specific anti-viral drug for treating the disease, timely detection of the disease and immediate treatment targeting symptoms presented by the infected individuals increases the chance of survival. For now, mass YF vaccination and effective vector control strategies are the popular measures been deployed to stem the menace of the disease [12].

Recent developments in epidemiological studies have shown that mathematical modelling played a significant role in the fight against infectious diseases and incessant disease outbreaks [6]. It has helped inform proactive health policies and unveil cost-effective control measures which, when implemented, could remarkably reduce the negative impacts of future disease outbreaks. Starting with earlier applications of mathematical modelling in epidemiology initiated by Sir Ross; several researchers have since applied modelling in the

spread and control of infectious diseases (See: [4, 10, 2, 9, 14, 1, 7, 8, 13, 3]). For example, Raimundo et al modelled the transmission dynamics of Yellow-fever in the presence of vaccine. Results from their study unveil some crucial threshold parameters which should be considered (for proper attention) in the design of YF control measures and vaccinations schedules in order to halt the spread of the disease, particularly in its endemic areas [8].

Also, Zhao et al modelled the recent YF outbreak in Luanda, Angola. Their model prediction fitted very well with weekly reported incidence and mortality resulting from the epidemic. One outstanding contribution from their work is that it gives a guidelines for assessing future outbreaks while also equipping the decision makers with likely action to take in order to minimize the attendant casualties. In addition, their findings provide criteria for evaluating future vaccination program [15]. In general, a review of mathematical models contributions to the control of neglected tropical infectious diseases emphasizes the need for collaborative research work across different disciplines (theoretical and field research) which will aid the evolution of data-driven model with economically implementable results that would drive policy decision making [6].

This paper is outlined as follows: The proposed mathematical model for the Yellow-fever transmission dynamics will be presented and it will be shown to be well-posed in section 2; the model will be qualitatively analyzed in section 3; the model will be numerically solved and simulations of the results will be carried out with findings from the simulations discussed in section 4; conclusions from the study will be given in the final section.

2 Proposed Mathematical Model

A deterministic mathematical model for the spread of Yellow-fever (YF) disease within the human and mosquitoes population is proposed with the assumption that the two populations mixes freely without barriers. The model subdivides the human population into five distinct compartments namely: the susceptible $S_h(t)$ which represents the density of the susceptible individuals, the exposed $E_h(t)$ which represents the density of the YF exposed individuals, the infected $I_h(t)$ which represents the density of the YF infected individuals, the Toxic -infected $T_h(t)$ which represents the density YF exposed individuals whose cases degenerate into the toxic one and the recovered $R_h(t)$ represents the density of the recovered and immune individuals. Similarly,

the mosquitoes population is subdivided into two compartments - the susceptible mosquitoes $S_v(t)$ which denotes the susceptible mosquitoes density and the YF-infected mosquitoes $S_v(t)$ denotes the infected mosquitoes density . It is important to mention here that the model does not make a distinction between the vaccinated humans and recovered humans since current YF vaccines now confer individuals with life-long immunity just as recovery from the infection [12]. Also, the propose model does not include contribution of the individuals in the toxic phase of the disease to the disease incidence because they no longer possess the viremia and as a result they are not infectious. [7] Thus, the proposed model is as presented below:

$$\begin{aligned}
 \frac{dS_h}{dt} &= b_h N_h + (1 - \rho)\Lambda - \lambda_{vh} - \epsilon S_h - \mu_h S_h \\
 \frac{dE_h}{dt} &= \lambda_{vh} - \gamma_h E_h - \mu_h E_h \\
 \frac{dT_h}{dt} &= (1 - \theta)\gamma_h E_h - \delta T_h - (\mu_h + \alpha)T_h \\
 \frac{dI_h}{dt} &= \theta\gamma_h E_h - \delta I_h - (\mu_h + \alpha)I_h \\
 \frac{dR_h}{dt} &= \delta T_h + \delta I_h + \rho\Lambda + \epsilon S_h - \mu_h R_h \\
 \frac{dS_v}{dt} &= b_v N_v - \lambda_{hv} - \mu_v S_v \\
 \frac{dI_v}{dt} &= \lambda_{hv} - \mu_v I_v
 \end{aligned} \tag{2.1}$$

where $\lambda_{vh} = \frac{a\beta_1 S_h I_v}{N_v}$, $\lambda_{hv} = \frac{a\beta_2 S_v I_h}{N_h}$ with the term $\lambda_{vh} = \frac{a\beta_1 S_h I_v}{N_v}$ denoting the rate at which susceptible individuals S_v get infected from the infected mosquitoes I_v while , $\lambda_{hv} = \frac{a\beta_2 S_v I_h}{N_h}$ denotes the rate at which susceptible mosquitoes S_V get infected from the infected human host I_H . The description of the parameters in the model are given in the Table 2.1 that follows:

Table 2.1: Description of parameters of the model system

Parameter	Description
β_1	transmission probability of YF disease from mosquitoes to human
β_2	transmission probability of YF disease from human to mosquitoes
γ_h	progression rate from E_h to I_h
b_h	Birth rate of Human
b_v	Birth rate of mosquitoes
a	daily biting rate
δ	recovery rate
α	YF induced-death rate for Human
ϵ	effective Vaccination rate of susceptible humans
ρ	proportion of Immigrant who are vaccinated
σ	Arrival rate of Immigrant per Individual per time
μ_h	Natural death rate for Human
μ_v	Natural death rate for Vector
Λ	Average Immigrants per unit time.
θ	Proportion of the E_h that deteriorate into the toxic case

Moreover, the total population sizes $N_h(t)$ and $N_v(t)$ can be determined by:

$$N_h(t) = S_h(t) + E_h(t) + T_h(t) + I_h(t) + R_h(t)$$

$$N_v(t) = S_v(t) + I_v(t) \tag{2.2}$$

Also, the summation of the differential equations in the model system for the human host population and vector population yields:

$$\frac{dN_h}{dt} = \Lambda + (b_h - \mu_h)N_h - \alpha I_h - \alpha T_h \tag{2.3}$$

$$\frac{dN_v}{dt} = (b_v - \mu_v)N_v \tag{2.4}$$

Based on equations (2.3) and (2.4), $N_h(t) \leq \frac{\Lambda}{b_h - \mu_h}$ and $N_v(t) \leq N_v(0)exp^{(b_v - \mu_v)t}$. However, it is worthy to note that total mosquitoes population N_v is stationary for $b_v = \mu_v$, declines for $b_v < \mu_v$ and grows exponentially for $b_v > \mu_v$.

Lemma 1 *Given that the initial conditions for the proposed model (2.1) lie in Ω , where*

$$\Omega = \{(S_h, E_h, T_h, I_h, R_h, S_v, I_v) \in \mathbb{R}_+^7 | S_h \geq 0, E_h \geq 0, T_h \geq 0, I_h \geq 0, R_h \geq 0, S_v \geq 0, I_v \geq 0\},$$

then there exists a unique solution for (2.1) and the solution remains in Ω for all time $t \geq 0$.

Proof

Considering the fact that the right-hand side of the model (2.1) are continuous and it also has continuous partial derivatives in Ω , it can be deduce that the model (2.1) has unique solution which exists for all time $t \geq 0$. Consequently, we only need to show that $S_h \geq 0$, $E_h \geq 0$, $T_h \geq 0$, $I_h \geq 0$, $R_h \geq 0$, $S_v \geq 0$, and $I_v \geq 0$ for all future time t .

Suppose $t_1 = \sup\{t > 0 | S_h \geq 0, E_h \geq 0, T_h \geq 0, I_h \geq 0, R_h \geq 0, S_v \geq 0, I_v \geq 0, \in [0, t]\}$.

Using the first equation in model (2.1), we have

$$\frac{dS_h}{dt} = b_h N_h + (1 - \rho)\Lambda - \lambda_{vh} - \epsilon S_h - \mu_h S_h \quad (2.5)$$

The above equation can be rewritten in the form

$$\frac{dS_h}{dt} + (K(t) + \epsilon + \mu_h)S_h = Z(t) \quad (2.6)$$

with $K(t) = \frac{a\beta_1 I_v}{N_v}$ and $Z(t) = b_h N_h + (1 - \rho)\Lambda$.

So,

$$\frac{d}{dt}(S_h(t) \exp\{(\epsilon + \mu_h)t + \int_0^t (K(\tau))d\tau\}) = Z(t) \exp\{(\epsilon + \mu_h)t + \int_0^t (K(\tau))d\tau\}.$$

On integration, the preceding equation becomes

$$S_h(t_1) \exp\{(\epsilon + \mu_h)t_1 + \int_0^{t_1} K(\tau)d\tau\} - S_h(0) = \int_0^{t_1} Z(\psi) \exp\{(\epsilon + \mu_h)\psi + \int_0^\psi K(\eta)d\eta\}d\psi$$

Therefore,

$$\begin{aligned} S_h(t_1) &= S_h(0) \exp\{-(\epsilon + \mu_h)t_1 + \int_0^{t_1} K(\tau)d\tau\} \\ &\quad + \exp\{-(\epsilon + \mu_h)t_1 + \int_0^{t_1} K(\tau)d\tau\} \times \int_0^{t_1} Z(\psi) \exp\{(\epsilon + \mu_h)\psi + \int_0^\psi Z(\eta)d\eta\}d\psi \\ &\geq 0 \end{aligned} \quad (2.7)$$

Similarly, it can be shown that $E_h \geq 0$, $T_h \geq 0$, $I_h \geq 0$, $R_h \geq 0$, $S_v \geq 0$, and $I_v \geq 0$. Hence, the proof to the lemma is complete. \square

The above them is necessary because it guarantees the uniqueness of the model solution and also that the model does not predict negative values for the population in each of its compartments.

Dimensional Transformation

Using the assumption that the human and the mosquitoes population do not change significantly during the time interval under consideration, the total population for each of the two subgroups (i.e. the human and the mosquitoes population) is taken to be a relative constant. Hence, without any loss of generality, the model can be normalized by scaling the population in each of the compartments by the total species population. This is done using the following transformation:

$s_h = \frac{S_h}{N_h}$, $e_h = \frac{E_h}{N_h}$, $t_h = \frac{T_h}{N_h}$, $i_h = \frac{I_h}{N_h}$, $r_h = \frac{R_h}{N_h}$, $s_v = \frac{S_v}{N_v}$, $i_v = \frac{I_v}{N_v}$ in the classes $S_h, E_h, T_h, I_h, R_h, S_v, I_v$ populations respectively. Also, taking $\sigma = \frac{\Lambda}{N_h}$ as the proportional arrival rate of immigrants per unit time; the model becomes:

$$\begin{aligned}
 \frac{ds_h}{dt} &= b_h + \sigma(1 - \rho) - a\beta_1 s_h i_v - \epsilon s_h - \mu_h s_h, \\
 \frac{de_h}{dt} &= a\beta_1 s_h i_v - \gamma_h e_h - \mu_h e_h, \\
 \frac{dt_h}{dt} &= (1 - \theta)\gamma_h e_h - \delta t_h - (\mu_h + \alpha)t_h \\
 \frac{di_h}{dt} &= \theta\gamma_h e_h - \delta i_h - (\mu_h + \alpha)i_h, \\
 \frac{dr_h}{dt} &= \rho\sigma + \delta t_h + \delta i_h + \epsilon s_h - \mu_h r_h, \\
 \frac{ds_v}{dt} &= b_v - (a\beta_2 s_v i_h) - \mu_v s_v, \\
 \frac{di_v}{dt} &= a\beta_2 s_v i_h - \mu_v i_v
 \end{aligned} \tag{2.8}$$

Thus, the solutions of the model can be restricted to the hyperplanes $s_h + e_h + t_h + i_h + r_h = 1$ and $s_v + i_v = 1$. The model system (2.8) monitors the proportion of the human and mosquitoes (vector) populations in each the designated compartments as time evolves with all state variables and parameters of the model taking to be non-negative for all $t \geq 0$. As a result, the model will be analyzed in a suitable feasible region where it is biologically meaningful and mathematically well-posed. This region is defined as below:

$$\Omega_1 = \{(s_h, e_h, t_h, i_h, r_h, s_v, i_v) \in \mathbb{R}_+^7 \mid s_h + e_h + t_h + i_h + r_h \leq 1, s_v + i_v \leq 1\}$$

3 Qualitative Analysis

In order to foresee the long term behavior of the modelled system, the model equilibrium solutions will be determined and the conditions for their stability shall be established. Thus, the model equilibrium solutions are obtained by

setting the right-hand side of each of the equation to zeros and solving the resulting system of equations simultaneously. However, the resulting system of equations need only be solved for five out the seven variables, since the remaining two can be obtained from the relation $s_h = 1 - (e_h + t_h + i_h + r_h)$ and $s_v = 1 - i_v$. As a result, the solution yields :

(i) The Disease-free equilibrium \mathcal{E}^0 : $(e_h^0 = 0, t_h^0 = 0, i_h^0 = 0, r_h^0 = \frac{\rho\sigma + \epsilon}{\mu + \epsilon}, i_v^0 = 0)$

(ii) The endemic equilibrium \mathcal{E}^* : $e_h^* = \frac{(\mu_h + \delta + \alpha)N}{\gamma\theta D} (\mathcal{R}_0 - 1)$

$$t_h^* = \frac{(1-\theta)N}{D\theta} (\mathcal{R}_0 - 1), \quad i_h^* = \frac{1}{D} (\mathcal{R}_0 - 1),$$

$$r_h^* = (\mu_h + \delta + \alpha)(\alpha + \mu_h) [a\gamma\beta_2\theta(\rho\sigma + \epsilon) + \gamma\mu_v\delta(\theta - \theta\sigma - 1) + \mu_v\epsilon(\gamma + \mu_h + \alpha + \delta)] + \alpha a^2\beta_1\beta_2\theta [\rho\sigma(\gamma + \mu_h + \alpha + \delta) + \gamma\delta(\theta\sigma + 1 - \theta)] \times \frac{1}{\gamma\theta D},$$

$$i_v^* = \frac{1}{D_1} (\mathcal{R}_0 - 1);$$

$$\text{where } \mathcal{R}_0 = \frac{(\gamma a^2 \beta_1 \beta_2 \theta)(\mu_h - \rho\sigma)}{\mu_v(\mu_h + \epsilon)(\mu_h + \delta + \alpha)(\gamma + \mu_h)}, \quad N = \mu_h \mu_v (\mu_h + \delta + \alpha) (\gamma + \mu_h),$$

$$D = a\beta_2 [\gamma a \beta_1 \theta \delta (\sigma - 1) + a\beta_1 \mu (\mu + \alpha + \delta) + a\beta_1 \gamma (\mu + \delta) + (\mu + \epsilon)(\gamma + \mu)(\mu + \alpha + \delta)],$$

$$D_1 = a\gamma\beta_2\theta(\mu_h - \rho\sigma) + \mu_v [\gamma\delta(1 + \theta\sigma - \theta) + \mu_h(\gamma + \mu_h + \alpha + \delta)].$$

It is imperative to mention here that the basic reproduction number (\mathcal{R}_0) is an important epidemiological quantity and it is defined as the average number secondary cases arising from a single infected individual during his/her infectious period when introduced into a completely susceptible host population [5, 11]. This threshold quantity provides insight on what needs to be done to curtail the spread of the disease.

Theorem 1 *The disease free equilibrium $\mathcal{E}^0 = (e_h^0 = 0, t_h^0 = 0, i_h^0 = 0, r_h^0 = \frac{\rho\sigma + \epsilon}{\mu + \epsilon}, i_v^0 = 0)$ is locally asymptotically stable, whenever $\mathcal{R}_0 < 1$.*

Proof

In order to establish local stability of this equilibrium, the Jacobian Matrix for the reduced - simplified model (2.8) which is our model with the exclusion of equations for s_h and s_v gives :

$$J = \begin{bmatrix} -a_{11} - \mu_h - \gamma & -a_{11} & -a_{11} & -a_{11} & a\beta_1 s_h \\ (1 - \theta)\gamma & -(\delta + \mu_h + \alpha) & 0 & 0 & 0 \\ \theta\gamma & 0 & -(\delta + \mu_h + \alpha) & 0 & 0 \\ -\epsilon & \delta - \epsilon & \sigma\delta - \epsilon & -(\epsilon + \mu) & 0 \\ 0 & 0 & a\beta_2(1 - I_v) & 0 & -a_{55} - \mu_v \end{bmatrix} \quad (3.1)$$

with $s_h = 1 - (e_h + t_h + i_h + r_h)$, $a_{11} = a\beta_1 i_v$, $a_{55} = a\beta_2 i_h$.

Thereafter, the Jacobian matrix is evaluated at the disease-free equilibrium (\mathcal{E}^0) to obtain :

$$J_{\mathcal{E}^0} = \begin{bmatrix} -\mu_h - \gamma & 0 & 0 & 0 & a\beta_1(1 - W) \\ (1 - \theta)\gamma & -(\delta + \mu_h + \alpha) & 0 & 0 & 0 \\ \theta\gamma & 0 & -(\delta + \mu_h + \alpha) & 0 & 0 \\ -\epsilon & \delta - \epsilon & \sigma\delta - \epsilon & -(\epsilon + \mu) & 0 \\ 0 & 0 & a\beta_2 & 0 & -\mu_v \end{bmatrix} \quad (3.2)$$

where $W = \frac{\rho\sigma + \epsilon}{\mu + \epsilon}$. The above matrix (3.2) has eigenvalues of $\lambda_1 = -(\epsilon + \mu) < 0$ and $\lambda_2 = -(\delta + \mu_h + \alpha) < 0$ while the remaining eigenvalues can be obtained from the sub-matrix below:

$$J_{Sub} = \begin{bmatrix} -\mu_h - \gamma & 0 & a\beta_1(1 - W) \\ \theta\gamma & -(\delta + \mu_h + \alpha) & 0 \\ 0 & a\beta_2 & -\mu_v \end{bmatrix} \quad (3.3)$$

The characteristic polynomial of the sub-matrix (3.3) is

$$\lambda^3 + c_1\lambda^2 + c_2\lambda + c_3;$$

with $c_1 = \gamma + 2\mu_h + \mu_v + \alpha + \delta > 0$,

$c_2 = (\delta + \mu_h + \alpha)(\gamma + \mu_h) + \mu_v(\gamma + 2\mu_h + \alpha + \delta) > 0$,

$c_3 = a_2\gamma\beta_1\beta_2(W - \theta) + \mu_v(\gamma + \mu_h)(\delta + \mu_h + \alpha) > 0$ if $\mathcal{R}_0 < 1$. In addition, $c_1c_2 - c_3 > 0$ whenever $\mathcal{R}_0 < 1$. Based on Routh-Hurwitz criteria for a polynomial of third degree, the real part of each of the eigenvalues of the sub-matrix (3.3) are all negative. Consequently, the disease-free equilibrium \mathcal{E}^0 is locally asymptotically stable, whenever $\mathcal{R}_0 < 1$. \square

4 Numerical Solution and Discussions

Using the initial conditions $s_h(0) = 0.62$, $e_h(0) = 3.4 \times 10^{-2}$, $t_h(0) = 6 \times 10^{-3}$, $i_h(0) = 4 \times 10^{-2}$, $r_h(0) = 0.3$, $s_v(0) = 0.95$, and $i_v(0) = 0.5$ with parameter values in Table 4.1, the model is solved numerically using the fourth order Runge Kutta scheme.

Table 4.1: Model parameter values, units and their sources

Parameter	Value	Unit/Remark	Source
β_1	0.6	per bite	[8]
β_2	0.5	per bite	[15]
γ_h	0.31	day^{-1}	Estimated and [12]
θ	15%	per population	[15]
b_h	4.94×10^{-5}	day^{-1}	Estimate
b_v	0.051	day^{-1}	Estimate and [15]
a	3.0	per vector per day	Estimate
δ	0.143	day^{-1}	[8]
α	3.5×10^{-1}	day^{-1}	[8]
ϵ	0.01	day^{-1}	Estimate and [15]
ρ	50%	day^{-1}	Estimate
σ	1.0×10^{-6}	day^{-1}	Estimate
μ_h	4.94×10^{-5}	day^{-1}	Estimate and [12]
μ_v	0.051	day^{-1}	Estimate and [15]

It is imperative to mention here that the above set of parameters values gives a basic reproduction number (\mathcal{R}_0) ranging from 0.17 – 4.24 depending on the value of $a \in [1, 5]$.

Thereafter, we simulate the model for different scenarios of the disease outbreak and discuss our findings.

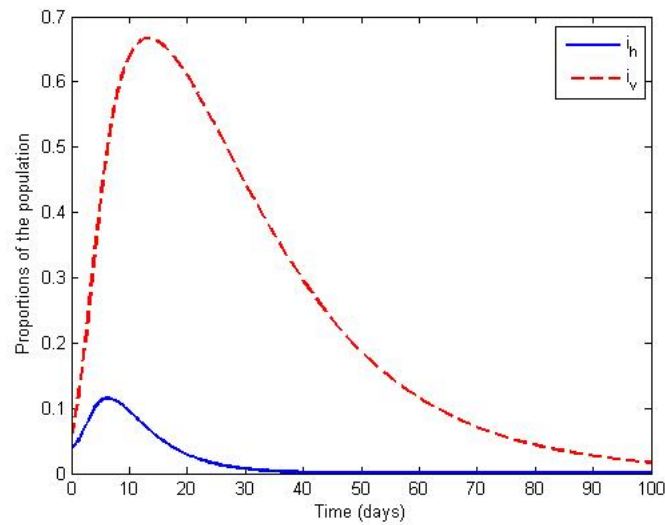


Figure 4.1: Profile of the $i_h(t)$ and $i_v(t)$.

Figure 4.1 shows that as the proportion of infected mosquitoes increase, the proportion of YF infected individuals also increase and the converse is also true. However, the proportion of the infected mosquitoes is always more than the proportion of infected humans over time. The implication is that any control measure which could help reduce the population of mosquitoes (particularly the Yellow fever infected ones) would be useful in reducing the proportion of humans infected with Yellow fever.

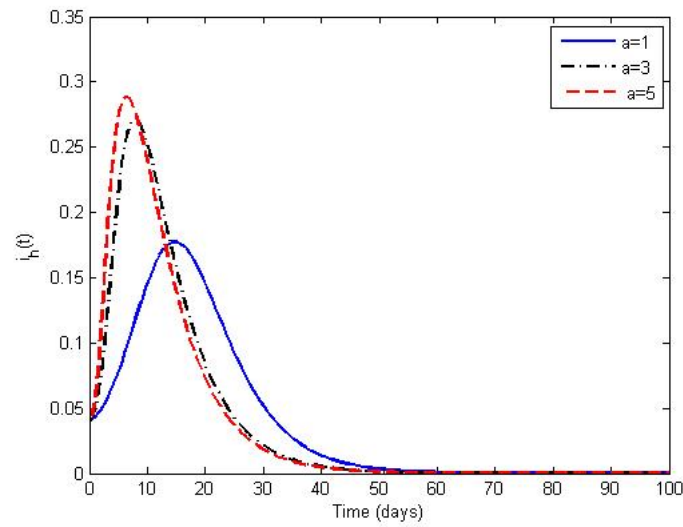


Figure 4.2: Profile of the $i_h(t)$ with varying mosquitoes biting rate a .

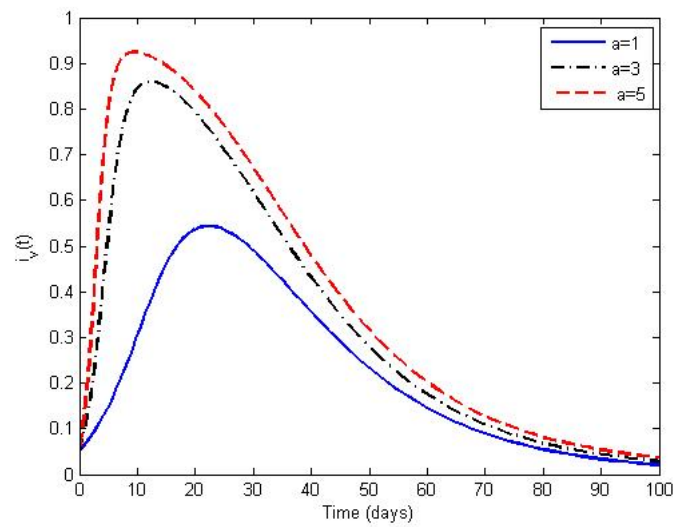


Figure 4.3: Profile of the $i_v(t)$ with varying mosquitoes biting rate a .

Figures 4.2 and 4.3 show that as the mosquitoes biting rate a increases, the proportion of the YF-infected human and mosquitoes population rise sharply, though fall gradually afterwards. It can be inferred that if the

breeding environment of the mosquitoes can be modified (or changed) by using biological plants whose presence in the environment hinders the breeding of mosquitoes and weakens their biting tendency, then the proportion of infected mosquitoes and humans will be reduced significantly. Another alternative towards reducing the mosquitoes biting rate is through the fumigation of potential mosquitoes breeding sites in our environment with specially formulated insecticides which could totally halt the mosquitoes reproduction cycle, and where this is not possible, the young mosquitoes developing from such process should be defective with minimal biting tendency. These suggestions, if actualized, could help reduce the proportion of the human and mosquitoes population that is infected with Yellow fever.

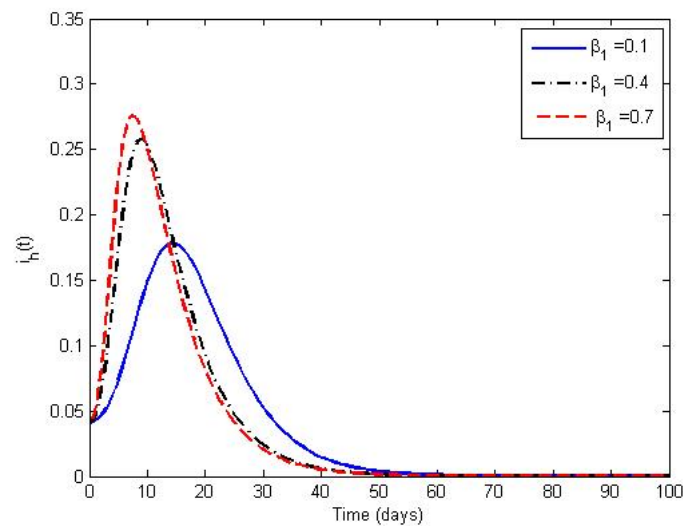


Figure 4.4: Profile of the $i_h(t)$ with varying values of β_1 .

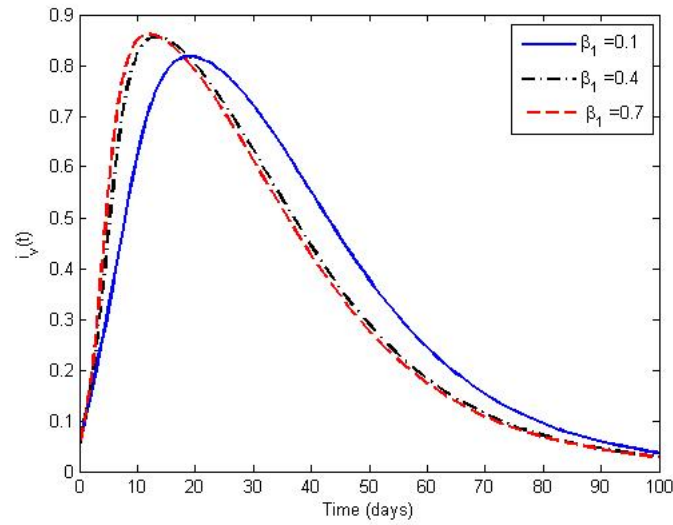


Figure 4.5: Profile of the $i_v(t)$ with varying values of β_1 .

Figure 4.4 indicates that as β_1 is increasing, the proportion of YF-infectious individuals continues to rise with peak attained in each cases getting higher as β_1 is getting bigger. Nevertheless, the higher the peak attained in each of these cases, the quicker the fall in the proportion of individual in this compartment after attaining the peak. However, there is in remarkable difference in the profile of $i_v(t)$ for varying values of β_1 as shown in Figure 4.5, except where the value of β_1 is significantly very low. This may not be unconnected with the fact that β_1 does not affect the dynamics of the infected mosquitoes directly. That notwithstanding, the use of mosquito nets and repellent are some measures that could help reduce the probability of transmission of YF from mosquitoes to human

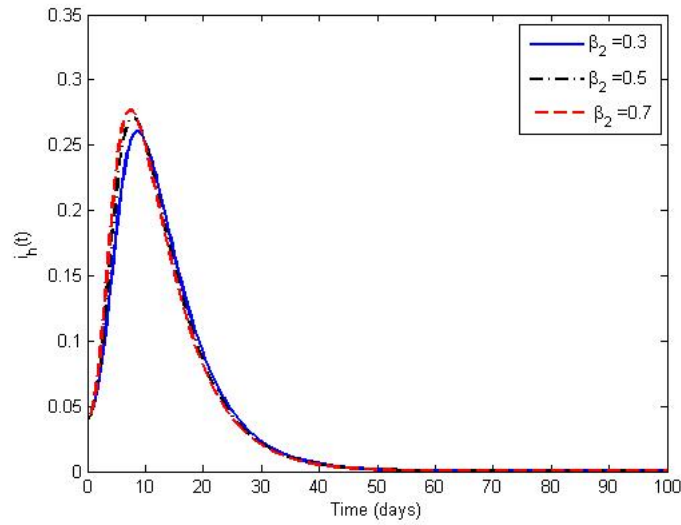


Figure 4.6: Profile of the $i_h(t)$ with varying values of β_2 .

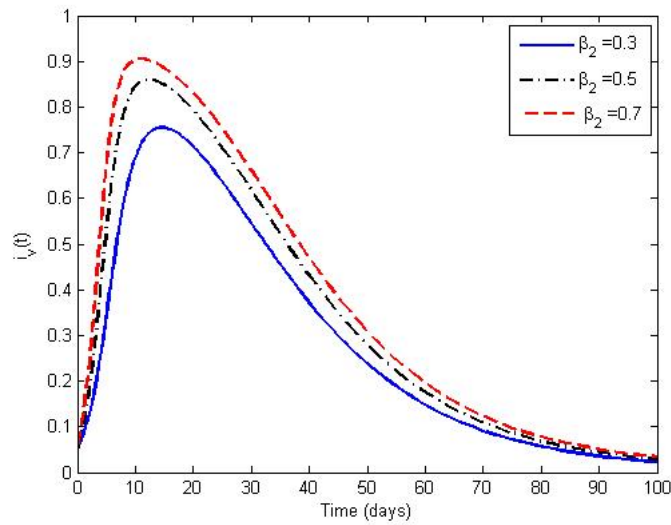


Figure 4.7: Profile of the $i_v(t)$ with varying values of β_2 .

Similarly, Figures 4.6 and 4.7 indicates dynamics of the infectious human and infected mosquitoes as the probability of transmission of YF from human to mosquitoes (β_2) changes. It is observed that the proportion of infected

mosquitoes rises as (β_2) increases, though this does not have significant impact on the proportion infected humans. In terms of measures that could be adopted to reduce (β_2) , adopting measures that disrupt contact between human and mosquitoes should suffice.

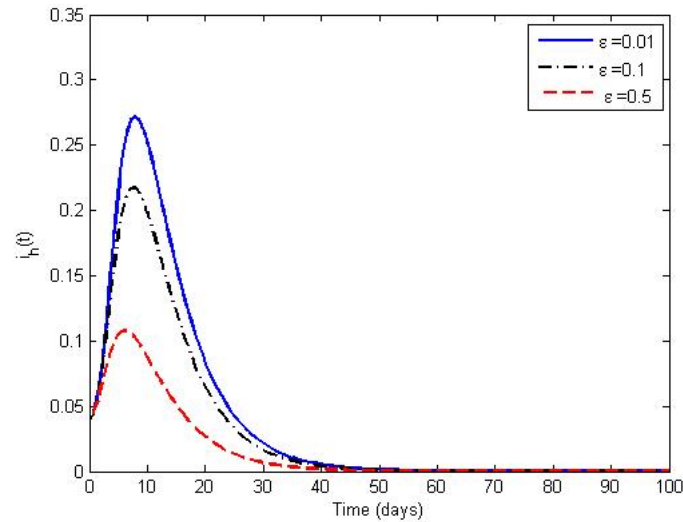


Figure 4.8: Profile of the $i_h(t)$ with varying values of ϵ .

In Figure 4.8, it is observed that as the vaccination success rate (ϵ) is increasing, the proportion of the YF infected human is also increasing. Moreover, the figure show that the proportion of the infected human peaked at about a tenth of the population before it begins to fall while this proportion tends to zero in about forty five days. This implies that if the vaccination coverage could be scaled up appropriately with the use of highly effective vaccines , YF outbreaks could be successfully contained in about fifty days.

5 Conclusion

A Mathematical model for the transmission dynamics of Yellow fever disease is considered. The model takes into consideration two sub-populations: the human population and the vector (mosquitoes) population. The model equilibrium solutions were obtained and the conditions for their local stability were established. A numerical solution to the model was obtained using forth order Runge-Kutta scheme and the results were simulated for different

scenarios of the disease situation. Our simulations show that control measures which reduce the mosquito biting rate, the human-vector transmission rate as well as vector-human transmission rate, and increase the vaccination success rate will be effective in curtailing the spread of the disease. Hence, control measures that address these identified factors (disease transmission parameters) would be useful in the strive towards the eradication of the disease.

References

- [1] Amaku M., Coutinho F. A., Raimundo S. M., Lopez L. F. , Burattini M. N. , and Massad E. (2014). *A comparative analysis of the relative efficacy of vector-control strategies against dengue fever*. Bulletin of Mathematical Biology, 76(3): 697 - 717.
- [2] Barrett A. D. and Higgs S. (2007) *Yellow fever: a disease that has yet to be conquered*. Annual Review of Entomology, 52: 209 - 229.
- [3] Ijalana C. O. and Yusuf T.T. (2017). *Optimal control Strategy for Hepatitis B Virus Epidemic in Areas of High Endemicity*. International Journal of Scientific and Innovative Mathematical Research, 5(12): 28 - 39.
- [4] Kermack WO, McKendrick AG.(1927), Contribution to the mathematical theory of epidemics. Proc. Royal Society London, A Contain Pap Math Phys Character.115:700?21. doi: 10.1098/rspa.1927.0118.
- [5] Kung'aro M. , Luboobi L. S. and Shahada F. (2014). *Reproduction number for Yellow Fever Dynamics Between Primates and Human Beings*. Commun. Math. Biol. Neurosci. 1 (5), 1-24.
- [6] Luz P.M., Struchiner C.J. and Galvani A.P. (2010) Modeling Transmission Dynamics and Control of Vector-Borne Neglected Tropical Diseases. PLoS Negl Trop Dis 4(10): e761. doi:10.1371/journal.pntd.0000761
- [7] Monath T.P, and Vasconcelos P.F (2015). *Yellow fever*. Journal of Clinical Virology, 64: 160 - 73. <https://doi.org/10.1016/j.jcv.2014.08.030>
- [8] Raimundo S.M., Amaku M. and Massad E. (2015). *Equilibrium Analysis of a Yellow Fever Dynamical Model with Vaccination*. Computational and Mathematical Methods in Medicine. <http://dx.doi.org/10.1155/2015/482091>

- [9] Raimundo S. M. , Yang H. M. , and Engel A. B. (2007). *Modelling the effects of temporary immune protection and vaccination against infectious diseases*. Applied Mathematics and Computation, 189(2): 1723 - 1736.
- [10] Ross R. (1916). *An application of the theory of probabilities to the study of a priori pathometry*. Proc Royal Society London, A 92: 204 - 230.
- [11] Van den Driessche P. and Watmough J. (2002). *Reproduction numbers and sub threshold endemic equilibria for compartmental models of disease transmission* Mathematical Biosciences, 180: 29 - 48.
- [12] World Health Organization (2018). *WHO factsheet on Yellow-fever*. Retrieved May, 2018 from <https://www.who.int/en/news-room/factsheets/detail/yellow-fever>
- [13] Wu J.T, Peak C.M, Leung G.M, and Lipsitch M. (2016). *Fractional dosing of yellow fever vaccine to extend supply: a modelling study*. Lancet. [https://doi.org/10.1016/S0140-6736\(16\)31838-4](https://doi.org/10.1016/S0140-6736(16)31838-4)
- [14] Yusuf T.T. and Benyah B. (2012). *Optimal control of vaccination and treatment for an SIR epidemiological model*. World Journal of Modelling and Simulation, 8(3): 194 - 204.
- [15] Zhao S., Stone L., Gao D., and He D. (2018) *Modelling the large-scale yellow fever outbreak in Luanda, Angola, and the impact of vaccination*. PLoS Negl Trop Dis 12(1): e0006158. <https://doi.org/10.1371/journal.pntd.0006158> .